Article (refereed) - postprint

Title: Space partitioning without territoriality in gannets

Authors: Ewan D. Wakefield[1]*[†], Thomas W. Bodey[2][†] , Stuart Bearhop[2], Jez Blackburn[3], Kendrew Colhoun[4], Rachel Davies[1], Ross G. Dwyer[2], Jonathan Green[5], David Grémillet[6,7], Andrew L. Jackson[8], Mark J. Jessopp[9], Adam Kane[8], Rowena H. W. Langston[10], Amélie Lescroël[6,11], Stuart Murray[12], Mélanie Le Nuz[13], Samantha C. Patrick[14][‡], Clara Péron[6], Louise Soanes[5], Sarah Wanless[15], Stephen C. Votier*[14], Keith C Hamer*[1]

Affiliations:

[1]School of Biology, University of Leeds, Leeds, LS2 9JT, UK.

[2]University of Exeter, School of Biosciences, Centre for Ecology & Conservation, Penryn, TR10 9EZ, UK.

[3]British Trust for Ornithology, The Nunnery, Thetford, IP24 2PU, UK.

[4]The Royal Society for the Protection of Birds, Northern Ireland Headquarters, Belvoir Park Forest, Belfast, BT8 4QT, UK

[5]School of Environmental Sciences, University of Liverpool, Environmental Sciences, Liverpool, L69 3GP, UK.

[6]CEFE-CNRS, 1919 route de Mende, F-34293 Montpellier Cedex 5, France.

[7]FitzPatrick Institute, DST/NRF Centre of Excellence, University of Cape Town, Rondebosch 7701, South Africa.

[8]Department of Zoology, School of Natural Sciences, Trinity College Dublin, Dublin 2, Ireland.

[9]Coastal & Marine Research Centre, University College Cork, Cork, Ireland.

[10]The Royal Society for the Protection of Birds, Sandy, Bedfordshire, SG19 2DL, UK.

[11]Biodiversité et gestion des territoires, Université de Rennes 1 – UMR 7204, Muséum National d'Histoire Naturelle, 35042 Rennes Cedex, France.

[12]Easter Craigie Dhu, Dunkeld, Perthshire, PH8 0EY, UK.

[13]Réserve naturelle des Sept-Iles, Ligue pour la Protection des Oiseaux, F-22560 Pleumeur Bodou, France.

[14]Marine Biology & Ecology Research Centre, Plymouth University, Plymouth, PL4 8AA, UK.

[15]Centre for Ecology & Hydrology, Penicuik, EH26 0QB, UK.

*Correspondence to: e.d.wakefield@leeds.ac.uk, stephen.votier@plymouth.ac.uk or k.c.hamer

† Contributed equally to this work.

Current address: ‡ Centre d'Etudes Biologiques de Chizé, CNRS-UPR1934, Villiers en Bois, France.

Abstract: Colonial breeding is widespread among animals. Some, such as eusocial insects, may use agonistic behavior to partition available foraging habitat into mutually exclusive territories; others, such as breeding seabirds, do not. We found that northern gannets, satellite-tracked from twelve neighboring colonies, nonetheless forage in largely mutually

exclusive areas and that these colony-specific home ranges are determined by density-dependent competition. This segregation may be enhanced by individual-level public information transfer, leading to cultural evolution and divergence among colonies.

Main Text: Colonial animals are constrained by their colony locations, which are ultimately limited by resource availability (*1*). However, within species, potential colony home ranges often overlap, implying competition among colonies may also be limiting (*2*). In eusocial central-place foragers the spatial effects of direct competition among colonies are well understood (*2*). In contrast, the spatial influences of indirect competition and information transfer on non-territorial species (e.g. seals, swallows and seabirds), where levels of relatedness are much lower, remain conjectural. For example, the hinterland model (*3*) predicts that breeding seabirds segregate along colonial lines, because of inequalities in travel costs from each colony. Predicted home ranges therefore comprise Voronoi polygons (Fig. 1A), as seen in some territorial animals (*2*). Food availability is assumed to be proportional to polygon area, limiting colony size. An alternative model proposes that density-dependent competition among colony members is limiting (*4*). As colonies grow, local prey depletion or disturbance requires birds to travel further to provision their young. However, this model ('Ashmole's halo') does not consider interactions among colonies and tacitly assumes that adjacent colonies' home ranges overlap (*5*).

Indirect evidence exists to support both models (*3, 6, 7*) and recent tracking studies suggest that seabirds and pinnipeds segregate along colonial lines (*8-12*). However, these studies proved inconclusive on the causes and ubiquity of segregation, largely because few colonies were sampled or tracking resolution was low. Here we use high resolution satellite-tracks of the foraging movements of 184 chick-rearing northern gannets *Morus bassanus* (hereafter gannets) from 12 of the 26 colonies fringing the British Isles (median 17 birds/colony), representing ~80% of the area's breeding population (Fig. 1A, Table S1), to test whether among-colony segregation occurs in a model colonial non-territorial central-place forager. We then use population- and individual-level models to explore potential mechanisms underlying spatial segregation.

Gannets are wide-ranging (max. foraging range ~700 km) pelagic seabirds that forage in patches of enhanced production, primarily on shoaling, mesotrophic fish and to a lesser extent fisheries discards (*13-15*). In almost all cases we tracked birds from adjacent colonies simultaneously (*16*). Individual gannet tracks (Figs. 1B and S1) and percentage Utilization Distributions (UDs, Figs. 2A and S2) showed a striking pattern of between-colony variation and spatial segregation, within and across years (Fig. S3). The size of 95% foraging UDs was strongly dependent ($F_{1,8} = 149.7$, $p < 0.001$, $R2 = 0.94$, Fig. S4) on square-root colony size (N). Likewise, maximum foraging range and trip duration were dependent on $N^{0.5}$ (Linear Mixed-Effects (LME) models, $p = 0.002$ and < 0.001, Tables S2 and S3). Birds from colonies of all sizes divided their time equally between foraging and chick attendance (LME, $p = 0.191$, Table S4) and the number of foraging trips/day was negatively dependent on $N^{0.5}$ (LME, $p = 0.024$, Table S5). Prey delivery rate, for which we assume trips/day is a proxy, is therefore negatively dependent on $N^{0.5}$, supporting the prediction that colony size is limited by density-dependent competition (*4, 6*). Contrary to the hinterland model (*3*), we found no relationship between colony Voronoi polygon area and colony size ($F_{1,35} < 0.01$, $p = 0.699$, $R^2 < 0.01$, Fig. S5).

Using empirical relationships between colony size and foraging area, we devised a population-level null model of the distribution of foraging gannets, assuming negligible competition between birds from neighboring colonies (*16*). This successfully explains among-colony segregation when colonies are far apart but predicts extensive overlap between

several study colonies, particularly in the Celtic Sea (Fig. 2A). However, observed UDs were largely mutually exclusive (Fig S2), overlapping markedly less than predicted (Fig. S6). For example, the null Population Overlap Index (POI, the number of potential pairwise interactions between birds from adjacent colonies(*16*)) for Little Skellig and Bull Rock (populations ~29,700 and 3700 pairs; separation distance 27 km) was 105,000, whereas the empirical estimate was 6000, largely because foraging trips were directed away from closely neighboring colonies (Fig. 1B). This pattern differs from the hinterland model in two key respects: segregation was not absolute and divisions between the UDs of unequally sized colonies were not equidistant between the two (Figs. 1B and S2) but typically occurred closer to the smaller colony, a phenomenon also observed in penguins (*9*). Hence the predictive performance of the hinterland model (log-likelihood, L = -0.54, AIC 3691, Table S6) was poor in comparison to the null model (L = -0.30, AIC = 2231).

Given the inability of existing models to explain gannet distribution when colonies are close together, we propose a multi-colony extension of Ashmole's halo (*4*), which we term the density-dependent hinterland (DDH) model. As adjacent colonies grow, foraging ranges increase due to prey depletion or disturbance (*6*) until their home ranges overlap. At low densities, birds from different colonies may forage together but as prey availability decreases populations respond by spreading down conspecific density gradients to the nearest areas subject to a lower rate of exploitation (*6*). As a first approximation, we assume a simple inverse relationship between the exploitation by conspecifics from adjacent colonies and the likelihood of new birds foraging in an area (*16*). However, the trade-off between transport and competition costs means birds favor areas close to their own colonies, so density declines with colony distance d (*10*). Hence, when colonies are large or close together segregation between home ranges may become absolute. Using these assumptions, we modeled the development of spatial segregation as colonies grow (*16*). We aim to replicate colony growth at the onset of the breeding season (*9*) but note that historical colony growth patterns may also influence spatial segregation (*6*), and that colony sizes are unlikely to be in equilibrium (*6, 14*). Initial comparisons with our tracking data showed that weighting the relative rate of exploitation by the $d^{0.5}$ improved this model, implying a decline in competitive fitness with distance. The DDH model proved a better fit to the tracking data (L = -0.58, AIC = 25440) than the null (L = -0.61, AIC = 27015, Table S7, c.f. Figs 2A and B). Furthermore, unlike the null, the DDH model successfully predicted the POI (Fig. 6) and the angular displacement of the centre of gravity of the 75% UDs from their colonies (circular correlation, observed vs. predicted directions, null model, r = 0.214, p = 0.463, n = 12; DDH model, r = 0.761, p = 0.020, n = 12).The shapes of the UDs predicted by the DDH model were closer to those observed (Dice's Similarity Coefficient s = 0.57, Table S8) than the null model's predictions (s = 0.45) (*16*). The DDH model's greater predictive strength was most marked for colonies with close neighbors (Fig.2, Table S8). Notably, the DDH model predicts greater foraging ranges than the null model (paired t-test, square-root mean distance t_{24} = 4.542, p < 0.001), implying that indirect competition from neighboring colonies diminishes chick provisioning rates, limiting colony size (*5*).

Like Ashmole's halo and the hinterland model, the DDH model assumes gannets are ideal free foragers. However, seabird prey occurs in widely dispersed, partially predictable patches (*17*). Thus seabirds may not base foraging decisions on personal information (memory) alone but may also exploit public information (*8, 18*), gained by observing conspecifics at the colony (*19-21*) or at sea (*22, 23*), although empirical evidence remains limited (*24*). To examine these hypotheses, we developed a range of 2D individual-based models of gannets foraging from two colonies (30 and 300 individuals), constrained by energy reserves (Table 1), to determine whether segregation emerges through information sharing (*16*). Only one

model, incorporating memory and public information transfer at sea and at the colony, produced a significant reduction in overlap between colony UDs (Figs. 3 and S7). Between-colony segregation rapidly became established and then persisted (Fig. S8), a pattern consistent at multiple food patch densities and most marked when colonies were close (Figs S9 and S10).

Public information is probably transmitted unintentionally, as in other colonial species (*18, 21, 23, 25, 26*). Several traits make this likely: Specifically, on arrival and departure from the nest, gannets signal visually and audibly. Prior to beginning foraging trips they land on the sea, near the colony, frequently departing in groups (*14*). These behaviors may allow conspecifics to follow or copy successful birds (*20, 21*), channeling information from the population to the individual, allowing birds to efficiently select foraging locations where they are competitively advantaged over conspecifics from other colonies. While these mechanisms are likely to operate over temporal scales of minutes to weeks, gannets have overlapping generations and a long pre-breeding period (≥ 4 years), during which they attend colonies with increasingly regularity (*14, 27*). This is thought to allow young birds to learn about prey distribution. If this involves public information acquisition, the preconditions exist for cultural evolution of foraging behavior over much longer time scales (*8, 28*).

Our results suggest that density-dependent competition, rather than territoriality, causes spatial segregation in a model colonial central-place forager. Although the mechanisms remain unclear, there is increasing recognition that non-territorial colonial central-place foragers utilize public information to inform decisions (*18, 21, 23, 25, 26, 28*). Contrary to the prevailing view, we predict that between-colony segregation is the norm when aggregations of animals such as bats, seals, bumblebees and birds occur at high densities (i.e. when colonies are clustered or large), forcing a re-examination of our understating of their foraging ecology.

References and Notes:

1. J. F. Wittenberger, G. L. J. Hunt, *The adaptive significance of coloniality in birds*. Farner, D. S., J. R. King and K. C. Parkes (1985), pp. 1-78.

2. E. S. Adams, *Annu. Rev. Ecol. Syst.* **32**, 277 (2001).

3. D. K. Cairns, *Am. Nat.* **134**, 141 (1989).

4. N. P. Ashmole, *Ibis* **103**, 458 (1963).

5. R. W. Furness, T. R. Birkhead, *Nature* **311**, 655 (1984).

6. S. Lewis, T. N. Sherratt, K. C. Hamer, S. Wanless, *Nature* **412**, 816 (2001).

7. K. H. Elliott *et al.*, *Auk* **126**, 613 (2009).

8. D. Grémillet *et al.*, *Mar. Ecol.-Prog. Ser.* **268**, 265 (2004).

9. D. G. Ainley *et al.*, *Ecol. Monogr.* **74**, 159 (2004).

10. E. D. Wakefield *et al.*, *Ecol. Monogr.* **81**, 141 (2011).

11. S. Wanless, M. P. Harris, *Colon. Waterbirds* **16**, 176 (1993).

12. A. M. M. Baylis, B. Page, S. D. Goldsworthy, *Mar. Ecol.-Prog. Ser.* **361**, 279 (2008).

13. K. C. Hamer *et al.*, *Mar. Ecol.-Prog. Ser.* **338**, 295 (2007).

14. B. Nelson, *The Atlantic gannet*. (Fenix Books Ltd., Great Yarmouth, UK, ed. 2nd, 2001).

15. S. C. Votier *et al.*, *J. Appl. Ecol.* **47**, 487 (2010).

16. Information on materials and methods is available on Science Online.

17. P. Fauchald, *Mar. Ecol.-Prog. Ser.* **391**, 139 (2009).

18. T. J. Valone, *Behavioral Ecology and Sociobiology* **62**, 1 (2007).

19. P. Ward, A. Zahavi, *Ibis* **115**, 517 (1973).

20. A. E. Burger, *Colon. Waterbirds* **20**, 55 (1997).

21. H. Weimerskirch, S. Bertrand, J. Silva, J. C. Marques, E. Goya, *Plos One* **5**, 8 (2010).

22. N. J. Buckley, *Am. Nat.* **149**, 1091 (1997).

23. E. D. Silverman, R. R. Veit, G. A. Nevitt, *Mar. Ecol.-Prog. Ser.* **277**, 25 (2004).

24. H. Richner, P. Heeb, *Advances in the Study of Behavior, Vol 24* **24**, 1 (1995).

25. M. Baude, E. Danchin, M. Mugabo, I. Dajoz, *Proc. R. Soc. London Ser. B* **278**, 2806 (2011).

26. D. K. N. Dechmann *et al.*, *Proc. R. Soc. London Ser. B* **276**, 2721 (2009).

27. S. C. Votier, W. J. Grecian, S. Patrick, J. Newton, *Mar. Biol.* **158**, 355 (2011).

28. E. Danchin, L. A. Giraldeau, T. J. Valone, R. H. Wagner, *Science* **305**, 487 (2004).

29. M. S. Coyne, B. J. Godley, *Mar. Ecol.-Prog. Ser.* **301**, 1 (2005).

30. R. A. Phillips, J. C. Xavier, J. P. Croxall, *Auk* **120**, 1082 (2003).

31. D. Nicholls, C. J. R. Robertson, M. D. Murray, *Notornis* **54**, 137 (2007).

32. B. J. McConnell, C. Chambers, M. A. Fedak, *Antarctic Science* **4**, 393 (1992).

33. M. D. Sumner. (2011). trip: Spatial analysis of animal track data. R package version 1.1-10.

34. Y. Ropert-Coudert *et al.*, *J. Avian Biol.* **40**, 380 (2009).

35. K. C. Hamer *et al.*, *J. Anim. Ecol.* **78**, 880 (2009).

36. S. Garthe, S. Benvenuti, W. A. Montevecchi, *Can. J. Zool.-Rev. Can. Zool.* **81**, 453 (2003).

37. C. Calenge, *Ecol. Model.* **197**, 516 (2006).

38. J. Fieberg, C. O. Kochanny, *J. Wildl. Manage.* **69**, 1346 (2005).

39. J. van Etten. (2012). gdistance: distances and routes on geographical grids. R package version 1.1-2.

40. M. Hasegawa, M. Tanemura, *Ann Inst Stat Math* **28**, 509 (1976).

41. D. Bates, M. Maechler, B. Bolker. (2011). lme4: Linear mixed-effects models using S4 classes. R package version 0.999375-42.

42. G. Aarts, M. MacKenzie, B. McConnell, M. Fedak, J. Matthiopoulos, *Ecography* **31**, 140 (2008).

43. J. Pinheiro, D. Bates, S. DebRoy, D. Sarkar. (2012). nlme: Linear and Nonlinear Mixed Effects Models. R package version 3.1-103.

44. U. Wilensky, in *http://ccl.northwestern.edu/netlogo/*. (Center for Connected Learning and Computer-Based Modeling, Northwestern University, Evanston, IL., 1999).

45. E. D. Wakefield, R. A. Phillips, J. Matthiopoulos, *Mar. Ecol.-Prog. Ser.* **391**, 165 (2009).

46. S. Wanless, S. Murray, M. P. Harris, *British Birds* **98**, 280 (2005).

47. S. Murray, *Scottish Birds* **31**, 220 (2011).

48. K. C. Hamer, R. A. Phillips, J. K. Hill, S. Wanless, A. G. Wood, *Mar. Ecol.-Prog. Ser.* **224**, 283 (2001).

49. W. J. Grecian *et al.*, *Biol. Conserv.* **156**, 43 (2012).

50. J. C. Haney, K. M. Fristrup, D. S. Lee, *Ornis Scandinavica* **23**, 49 (1992).

Fig. 1. Gannets tracked from colonies (**A**) around the British Isles forage in largely mutually-exclusive areas, despite their potential home ranges overlapping (red - study colonies, yellow - others). Home ranges predicted by the hinterland model (*3*) form Voronoi polygons, bounded by lines of equidistance between colonies (black lines). Satellite tracks from184 individuals (**B**) show that foraging birds direct their movements away from neighboring colonies. Data collected 2011, except St Kilda (SK) collected 2010. Grey lines -200 and 1000 m isobaths; LS - Little Skellig; TB - Bull Rock (mentioned in the text, Table S1 for colony details).

Fig. 2. Density-dependent competition within and between colonies explains large-scale among-colony segregation. Observed colony Utilization Distributions (**A**, colored polygons plus 95, 75, 50 and 25% UD contours) are largely mutually exclusive. This is at odds with the null model (predicted 75 and 95% UDs solid and dashed lines), which assumes density-dependent competition only within colonies, predicting broad overlap between some UDs. The Density-Dependent Hinterland (DDH) model (**B**) additionally assumes competition between colonies, providing a better fit to the tracking data.

Fig. 3. Individual-based simulations show that overlap between the Utilization Distributions (UDs) of two hypothetical colonies (**A**, solid lines/blue circle - large colony ; dashed lines/red circle - small colony) reduces (**B**) only when birds use private information and gain public information prior to departure and during foraging trips (see Table 1 for model rules). Isopleths - 50, 75 and 95% UDs. Results shown for 25 prey patches. Error bars show 95% CIs.

Table 1. Rules governing information use in individual-based models of foraging gannets (see Table S10 for details).

| Foraging rules	Description
Null	Birds forage randomly during each trip
Memory (ME)	Birds return to previously successful locations (private information)
Local Enhancement (ME+LE)	ME + uninformed birds may follow informed birds at sea (private and public information)
Information Centre (ME+IC)	ME + uninformed birds may follow informed birds from their colony (private and public information)
All Sources Combined (ME+LE+IC)	ME + Uninformed birds may follow informed birds from the colony and at sea (public and private information)

Fig. 1

A Observed plus null model

0 200 400 km

B DDH model

Fig. 2

A

Null Model   Memory   Local Enhancement

Memory +
Information Centre   All Information
Sources

B

D ◻25 km ◻90 km ◻180 km

Population Overlap Index (pairwise interactions)

Behavioural rules

Null   ME   ME+IC   ME+LE   ME+LE+IC
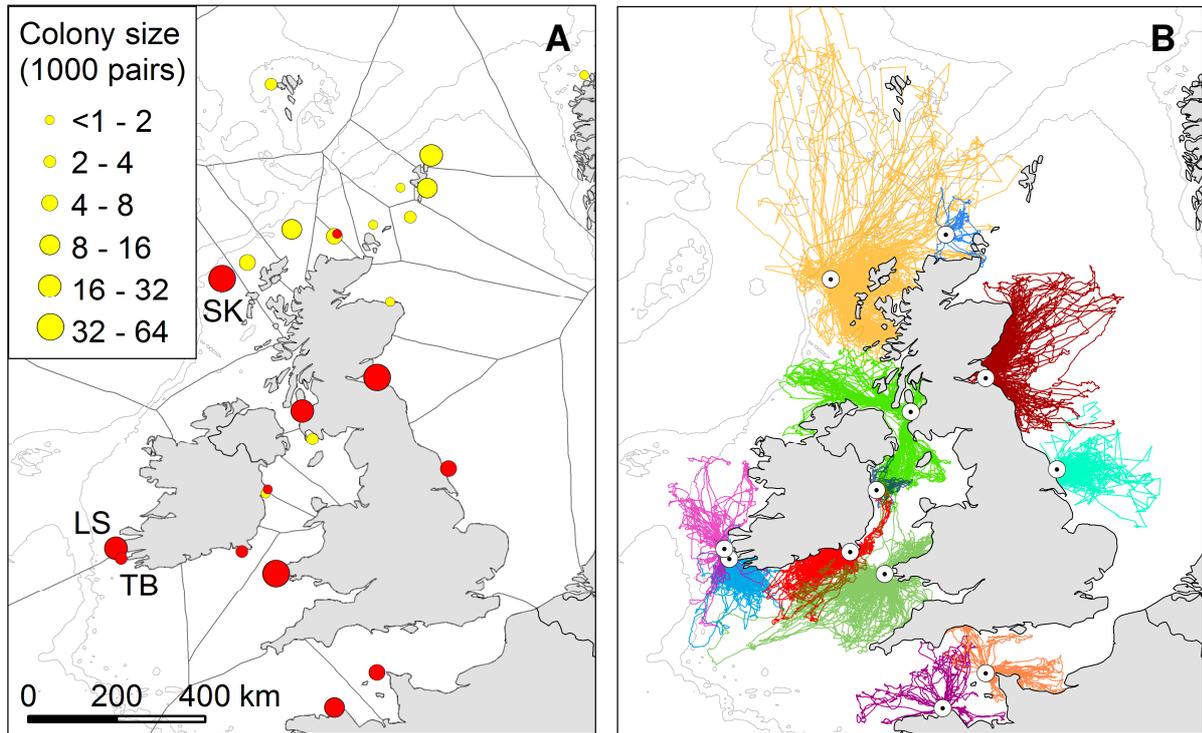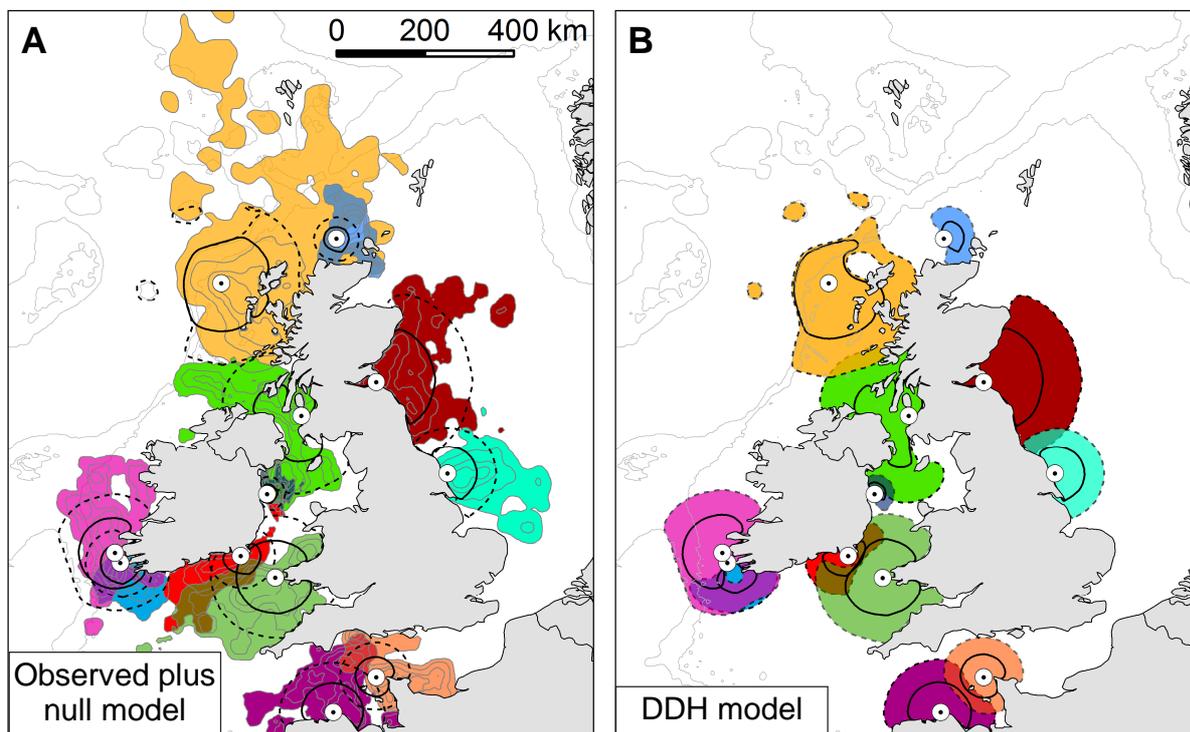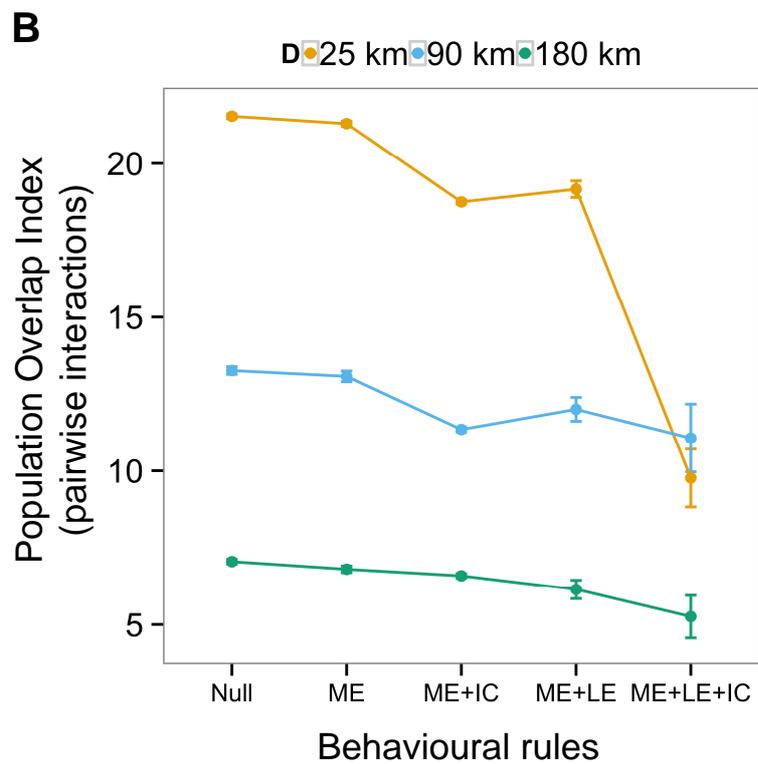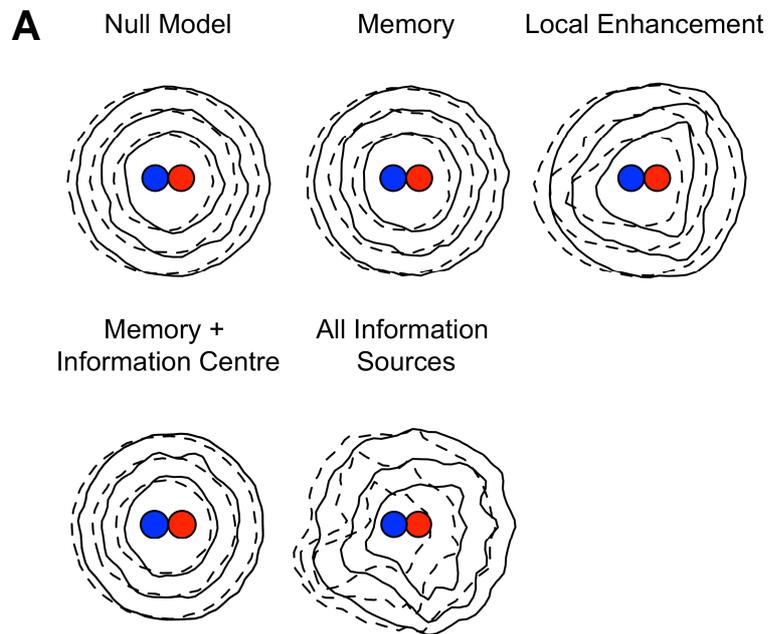
Fig. 3

Supplementary Materials for

Space partitioning without territoriality in gannets

Ewan D. Wakefield, Thomas W. Bodey , Stuart Bearhop, Jez Blackburn, Kendrew Colhoun, Rachel Davies, Ross G. Dwyer, Jonathan Green, David Grémillet, Andrew L. Jackson, Mark J. Jessopp, Adam Kane, Rowena H. W. Langston, Amélie Lescroël, Stuart Murray, Mélanie Le Nuz, Samantha C. Patrick, Clara Péron, Louise Soanes, Sarah Wanless, Stephen C. Votier, Keith C. Hamer.

correspondence to: e.d.wakefield@leeds.ac.uk

This PDF file includes:

Other Supplementary Materials for this manuscript:

Materials and Methods

Data collection

Birds were tracked while attending 2 - 5 week old chicks (trip duration was independent of chick age) from 11 colonies, between June and August 2011. Birds from four colonies were also tracked in 2010 and (due to logistical constraints) from St Kilda in 2010 only. Birds were approached at the nest on foot or by rope and caught using a metal crook or wire noose fitted to a 4-6 m pole or by hand. We then used a range of bird–borne devices to track gannets' foraging movements, choosing devices appropriate to logistical constraints imposed by the location and topography of each colony. On each bird one of the following tracking devices was deployed (for details see Table S1): a Platform Terminal Transmitter (PTT); a passive Global Positioning System (GPS) logger; or a GPS Radio Frequency (GPS-RF) logger. Locations from PTTs are received remotely via the ARGOS satellite system, whilst GPS loggers record positions onboard. However, while passive GPS loggers need to be recovered to download their data, GPS-RF loggers can be downloaded over a short-range (< 1 km) radio frequency link. Hence, we deployed PTTs at precipitous or very remote colonies (PTT - Kiwisat202, Sirtrack, Havelock North, New Zealand at St Kilda; PTT100 or LC4, Microwave Telemetry Inc at Bempton; 62, 45 and 40 g respectively). Location data for St Kilda were archived using the satellite-tracking and analysis tool (*29*). GPS-RF loggers were deployed at colonies where recapture was unlikely but remote download was possible from a boat or cliff top (GPS-RF, e-obs GmbH, Munich, Germany, 45 g). Passive GPS loggers were deployed at more easily accessible colonies (i-gotU GT-120 or i-gotU GT-200, Mobile Action Technology Inc., Taipei, Taiwan, 20 g and 37 g respectively; or CatTraQ, Perthold Engineering LLC, Anderson, USA, 18 g).

PTTs operated either in continuous transmission mode or duty cycled 1 hour on – 1 hour off (median resultant interval 75 minutes). GPS loggers recorded locations every 1 or 2 minutes. Auxiliary Time Depth Recorders (TDRs) were deployed simultaneously with tracking devices on birds from Bass Rock, Grassholm, Great Saltee and Île Rouzic. TDRs employed were either G5 or G6A loggers (CEFAS Technology, Lowestoft, UK, 2.5 g) or MSR145 loggers (MSR Electronics GmbH, Seuzach, Switzerland, 18 g). Devices were attached to the base of birds' ventral three tail feathers using Tesa tape (*8*). Birds were re-caught after 1 - 21 foraging trips and the loggers removed, with the exception of PTTs and GPS-RF tags. These remained attached until birds shed their central tail feathers, which are in active molt during the breeding season. Deployment and recovery times averaged 12 and 9 minutes respectively and after release, birds returned almost immediately to the nest.

In addition, during August 2010 and 2011, a number of breeding adult gannets were also fitted with a MK5, MK15 or MK19 combined light and immersion logger (British Antarctic Survey, Cambridge, UK, 3.6, 2.4 and 2.4 g respectively). These devices were attached to a metal ring placed around the tarsus of the bird's leg and recovered the following breeding season. MK5 and 15 loggers test whether the device is wet or dry every 3 seconds, recording the total number of samples wet every 10 minutes. The MK19 records the time of transition (3 second resolution) between wet/dry states providing the

new state lasts more than 6 seconds. In all cases, total instrument mass was ≤ 2% of body mass, below the maximum recommended for seabird biologging studies (*30*).

Tracking data filtering

The temporal resolution of GPS data was standardized to 2 minutes and locations in the colony were removed. Incompletely recorded trips were omitted from our analysis. The median error from the true position of GPS locations was 8 m so no further filtering was necessary. In contrast ARGOS data in location classes 3, 2, 1, 0, A and B received from PTTs attached to volant pelagic seabirds have mean error from true position of between 0.1 and 5.0 km (*31*). Hence, we filtered PTT tracks with an iterative forward/backward speed averaging algorithm (*32*), implemented in the R package 'trip' (*33*). Locations resulting in implausibly high travel speeds (>87 km/h, the 99th percentile of the speeds of GPS-tracked gannets) were removed, along with locations on land > 5 km from the coast. Contiguous locations greater than 5 km from the colony were assumed to be from foraging trips, while the remaining locations were deleted.

Discrimination of foraging behavior

Gannets primarily forage by plunge-diving during daylight (*34*). We therefore characterized foraging movement patterns by comparing GPS and TDR data (*8*). Daytime GPS locations meeting any of the following empirically determined criteria were assumed to be indicative of putative foraging: (1) tortuosity < 0.9 and speed > 1 m/s; (2) speed > 1.5 and < 9 m/s; or (3) tortuosity ≥ 0.9 and acceleration < -4 m/s^2. Speed and acceleration were calculated between L_{-1} and L_0, where L_0 is the focal location. Tortuosity is the ratio of the straight-line to along-track distance between L_{-4} and L_4. Validation of these criteria showed that, within individuals, 99% of GPS locations occurring within 10 minutes of dives detected using TDRs were classified as foraging. Conversely, 62% of GPS locations classified as foraging occurred within 10 minutes of dives (note that gannets frequently exhibit search behavior without diving (*35*). This methodology was used only for GPS-tracked birds, as the spatiotemporal resolution of PTT data was insufficient to discriminate foraging in this way. Hence, subsequent analyses that refer specifically to putative foraging locations exclude tracking data from St Kilda and Bempton.

Date of arrival at the colony

During the non-breeding period the vast majority of gannets leave the vicinity of their colonies and remain at sea (*14*). At the onset of the breeding season birds return to their colonies, making periodic foraging trips. During this time they spend the hours of darkness at rest, either on the surface of the sea or in their colonies (*36*). We therefore defined the date of arrival of adult birds at the colony after the winter period as the first night spent on land. For each bird fitted with an immersion logger we calculated the

3

proportion of each night during which the logger was dry. If this exceeded 0.9 the bird was deemed to have spent the night in the colony, allowing us to identify the date of first arrival in the colony at the onset of the breeding season.

Spatial usage and overlap

Utilization Distributions (UDs, i.e. the probability distribution defining each colony's use of space) were estimated by calculating the colony mean kernel density (KD) of (1) all locations and (2) putative foraging locations. Kernel Density (KD) was calculated on a 2 km Lambert Azimuthal Equal Area grid using the R package adehabitat (37). Because individuals were tracked for different lengths of time, we estimated KD for each individual, selecting the smoothing parameter h best describing the individual's distribution by least-squares cross-validation. We then averaged across individuals to estimate colony mean KD. This allowed the animals with fewer data points, and therefore higher smoothing bandwidths, to be represented by more diffuse distributions.

We defined overlap in spatial usage of birds from neighboring colonies using two indices. Firstly, the Home Range Overlap Index (HROI) was defined as the mean of the area of intersection divided by the area of each colony's estimated home range. Home range was defined at three probabilities of use ($p = 50$, 75 and 95%) by percentage UD contours, UD_p. Hence, the HROI between colonies i and j was:

$$\text{HROI} = 0.5\left(\frac{A(UD_{i,p} \cap UD_{j,p})}{A(UD_{i,p})} + \frac{A(UD_{i,p} \cap UD_{j,p})}{A(UD_{j,p})} \right), \qquad (1)$$

where $A(UD_{i,p})$ is the area of the ith colony's p percentage UD contour, etc. While this index is intuitively easy to interpret, it does not incorporate information on how bird density varies within home ranges (38). Hence, we also estimated space use sharing among birds from neighboring colonies using the following index, which we term the Population Overlap Index (POI):

$$\text{POI} = \sum_{\text{All } x} \hat{u}_{i,x} N_i \hat{u}_{j,x} N_j , \qquad (2)$$

where $\hat{u}_{i,x}$ is the estimated absolute density of use of cell x by the population of the ith colony and N_i is the size of the ith colony. This is similar to the Utilization Distribution Overlap Index commonly used to quantify overlap between the UDs of individuals (38) but incorporates information about relative population size. It may therefore be interpreted as the sum total of all potential pairwise interactions between birds from the two colonies. In the special case of UDs uniformly distributed about two equally sized colonies, square-root POI equals the expected number of birds from either colony utilizing the area of overlap between the two colonies' UDs. Throughout our analysis we use the most recent available estimates of gannet colony size N (Table S1).

Colony distance estimation

Gannets almost invariably avoid flying over land barriers (*14*) (Fig. 1B). Hence, the minimum distance they must fly to reach locations at sea from their colonies is greater than the straight line distance if there are any intervening land masses. We therefore used the shortest path distance avoiding land *d* throughout our analysis. The distance d_i from the *i*th colony to all cells at sea on a 2 km Azimuthal Equidistant projection grid was estimated using the R package gdistance (*39*). Movement from each cell was assumed to be possible to any cell in a 16 cell neighborhood.

Population-level models

Breeding gannets are almost exclusively neritic foragers (Fig. 2), so our analyses exclude waters > 1000 m deep. Distance d_i refers to the shortest path from the *i*th colony avoiding land. Voronoi polygons were defined by arranging remaining areas within the birds' maximum foraging range d_{max} (780 km, which is 1.1 x the maximum *d* observed in the study) in a Dirichlet tessellation of (*2, 40*). The probability density φ of foraging effort, assuming negligible competition from conspecifics from adjacent colonies (null model), was estimated using an R algorithm (see Supplementary Materials). In brief, this proceeds as follows: For the *i*th colony, A_i, the area of the 95% UD, and the mean μ_i and standard deviation σ_i of square-root foraging range are predicted by N_i using empirical relationships. Probability density is then estimated for each 4 km cell *x* in each 10 km wide distance bin *m* centered on distance $d_{i,m}$, according to the square-root normal probability density function (Fig S11):

$$\varphi\left(d\right)_{i,x,m} = \frac{1}{2 n_m \sigma_i \sqrt{2\pi}} \left| \frac{1}{\sqrt{d_{i,x,m}}} \right| e^{-\frac{1}{2\sigma_i^2}\left(\sqrt{d_{i,x}}-\mu_i\right)^2}, \tag{3}$$

where n_m is the number of cells in bin *m*. The area of the predicted 95% UD is then calculated. If this differs from A_i by more than 5%, μ_i and σ_i are adjusted by a small amount and the preceding steps repeated (this is necessary because the extent of accessible neritic waters differs between colonies).

To account for density-dependent competition among adjacent colonies (the density-dependent hinterland model), the algorithm was modified as follows: The density of foraging birds around a colony is dependent on colony size. Although we assume that spatial segregation develops as colonies grow during the breeding season, as reported by Ainley et al. (*9*) in Adélie penguins, historical colony growth patterns may have also influenced segregation (*6*). Our aim is not to test between these two hypotheses (which are not necessarily exclusive). Rather, we aim simply to demonstrate how density-dependent avoidance of birds from neighboring colonies can give rise to observed patterns of among-colony segregation. At the onset of the breeding season, birds are nominally assumed to return to the colony over a 60 day period, with arrival dates normally distributed (mean 30 days, sd = 10 days, see Fig. S12). Colony growth from zero to the observed maximum therefore follows a sigmoid curve described by the cumulative normal distribution function. Proceeding in *t* time steps colony size N_i is

5

increased incrementally according to this function, reaching its observed size at time $t = 20$ (i.e. one time step is equivalent to 3 days). At each time t the distance $d_{i,x}$ from colony i to each cell x is calculated, taking account of any cells excluded in preceding time steps (see below). Probability density φ is then estimated as described above. It is assumed that food availability is finite. Hence, as colony home ranges expand, the likelihood of gannets using a new location is also negatively dependent on the density of conspecifics from other colonies already using that location. We therefore make the arbitrary assumption that the probability of birds using a new location is inversely proportional to λ_p, the rate of exploitation by birds from the set of all other colonies $\{j = 1,2 \ldots, n, j \neq i\}$, weighted by the inverse of square-root colony distance. Above λ_{max} no new birds forage at a location. The probability density φ is therefore multiplied by p, where

$$p_{i,x,t} = \delta_{i,x,t}\left(1 - \frac{\lambda_{p,i,x,t-1}}{\lambda_{max}}\right), \text{ where } \delta_{i,x,t} = \begin{cases} 1 \text{ if } \lambda_{p,i,x,t-1} < \lambda_{max} \\ 0 \text{ otherwise} \end{cases} \qquad (4)$$

λ_p is passed from the preceding time step, t_{-1}:

$$\lambda_{p,i,x,t-1} = \sum_{\text{All } j \neq i} \frac{\varphi_{j,x,t-1} N_{j,t-1} \tau_{j,t-1}}{\sqrt{d_{j,x,t-1}}}, \qquad (5)$$

where $\tau_{j,t}$ is the predicted number of trips made per day, which is dependent on $N_{j,t}$. Cells where $\lambda_p > \lambda_{max}$ are made inaccessible to birds from the ith colony in subsequent time steps. The simplicity of equation 4 means that only one parameter, λ_{max}, is estimated by the model (Fig. S13). This is achieved by maximizing the log-likelihood, which is determined by cross-validation, as described below. The true form the density-dependent response of gannets to conspecifics from adjacent colonies may be more complex as it is likely to depend on local prey abundance, as well as conspecific facilitation, local enhancement and interference competition (6, 14). However, none of these factors are presently sufficiently well understood in gannets to make more detailed assumptions.

Model comparison and tests

Relative model performance was assessed by treating colony Voronoi polygons and predicted φ as explanatory covariates in a binomial generalized linear mixed model of spatial usage fit in the R package lme4 (41). Putative foraging locations were treated as presence data, which were matched with pseudo-absence locations, randomly selected from the area accessible to birds from each colony (10, 42). In order to account for unequal sample sizes and variation within birds and colonies, individual, nested within colony was treated as a random effect. Voronoi polygon was treated as a binary categorical covariate (either 'home' or 'foreign'). Model performance was compared in two steps: Initially, the coarse scale predictions of the hinterland model and the null model were assessed. In this instance, pseudo-absence locations were selected from the area within a distance of 1.1 x d_{max} from each colony. Having demonstrated that foraging area varies with colony size we then assessed the performance of models 1 and 2 at a

finer scale. For each colony, pseudo-absence locations were selected from within an area extending to 1.1 x the maximum foraging range predicted for that colony. Relative explanatory power was assessed by comparing AIC and log-likelihood L. The latter was determined by colony-level leave one out cross-validation, where

$$L_m = \frac{\sum_{i=1}^{n_m} \ln \left(\hat{u}_{m,i} \left(1 - h_{m,i}\right)^{1-\hat{u}_{m,i}} \right)}{n_m} \tag{6}$$

and $h_{m,i}$ and $\hat{u}_{m,i}$ are the ith prediction and observation and from the mth colony and n is the number of locations from that colony (*10, 42*).

The shape of the percentage UDs predicted by models 1 and 2 was compared to that observed by satellite-tracking using Dice's Similarity Coefficient s, where

$$s = \frac{2A(UD_o \cap UD_p)}{A(UD_o) + A(UD_p)}, \tag{7}$$

$A(UD_o)$ and $A(UD_p)$ are the areas of the observed and predicted UDs respectively and s ranges from 0 (no overlap) to 1 (observed and predicted UDs overlap completely).

The response of spatial usage covariates to colony size was modeled using either Generalized Linear Models or Linear Mixed-Effects models. In the latter, colony was treated as a random effect to account for unequal sample sizes from colonies and within-colony variation. Models were fitted using the R package nlme (*43*). Where appropriate the response was transformed and normality checked using q-q normal plots of the residuals. We considered p-values significant at the $\alpha = 0.05$ level.

Individual-based simulations

Simulations were undertaken in the individual-based multi-agent modeling environment Netlogo (*44*). Due to a lack of synoptic information on prey distribution and the impracticality of simulating the behavior of tens of thousands of individuals, we did not attempt to devise a comprehensive model of gannet foraging behavior. Rather, we aimed to determine whether simple but realistic rules governing information transfer produce between-colony segregation.

Simulated gannets foraged in two-dimensional space from two colonies differing in size by an order of magnitude (30 vs. 300 individuals). Individuals moved at a constant speed of 30 km/h, with each time step representing five minutes' model time. Model space was constrained through the use of an energy term. Individuals began trips with the same quantity of energy, which they lost at a rate of one unit lost per time step. Total initial energy was determined by time required to reach the maximum observed range of foraging gannets at typical flight speeds (Table S9). On returning to the colony,

individuals remained there for a log-normally distributed random interval, before departing on a new foraging trip.

All simulations were initiated with a fixed number of prey patches, randomly distributed in accessible foraging space. To mimic the semi-predictable locations of tidal fronts and other mesoscale structures believed to be important foraging habitats (*17, 45*), patches underwent a random walk, with step length drawn from a normal distribution (mean = 0, sd = 2). Patches became visible at a greater distance and had an increased probability of dispersing once discovered, mimicking predator aggregation and prey detection and escape behavior (*6, 17*). In addition, to mimic the random appearance and disappearance of prey patches in surface waters, at each time step there was a 1 in 1000 chance of patches relocating to another position in model space. Simulated gannets discovering a prey patch remained there until it disappeared, at which point they returned to their colony. Unsuccessful individuals returned when their energy reserve was exhausted (for other constraints see Table S9).

Depending on the behavioral rules invoked in a run of simulations, an individual's foraging state could change as a result of gaining private information, through interactions with conspecifics or encounters with prey. In the null model, individuals foraged randomly with simple local inhibition at high conspecific densities. Rules then became increasingly complex, incorporating both private and public information acquisition. One hundred simulations were run for each of five sets of behavioral rules (see Table 10 for details), four prey patch densities (5, 10, 20 or 50 patches) and three colony separation distances (25, 90 or 190 km). At the start of each simulation a burn-in period of 1000 iterations (where an iteration represents 5 minutes of model time) allowed movement patterns to become established. This step was necessary as simulations started with individuals in the unrealistic state of being uninformed about prey distribution. Each simulation was then run for two weeks of model time. Colony 95% UDs were calculated using the locations of foraging individuals sampled every 5 minutes and the HROI was calculated according to equation 1.

Supplementary Text

Fig. S1.

The degree of among-colony segregation is highlighted by the distribution of the terminal points of foraging trips made by tracked gannets (n = 184 individuals from 12 colonies, see Table S1 for details). Each color corresponds to a different colony. Grey lines indicate the 200 and 1000 m isobaths. Data shown are from 2011, except those from St Kilda from 2010. Colony names: AC - Ailsa Craig; BP - Bempton; BR - Bass Rock; CI - Les Etacs & Ortac; GH - Grassholm; GS - Great Saltee; IR - Île Rouzic; LB - Lambay; LS - Little Skellig; SK - St Kilda; SS - Sule Skerry; TB - Bull Rock.
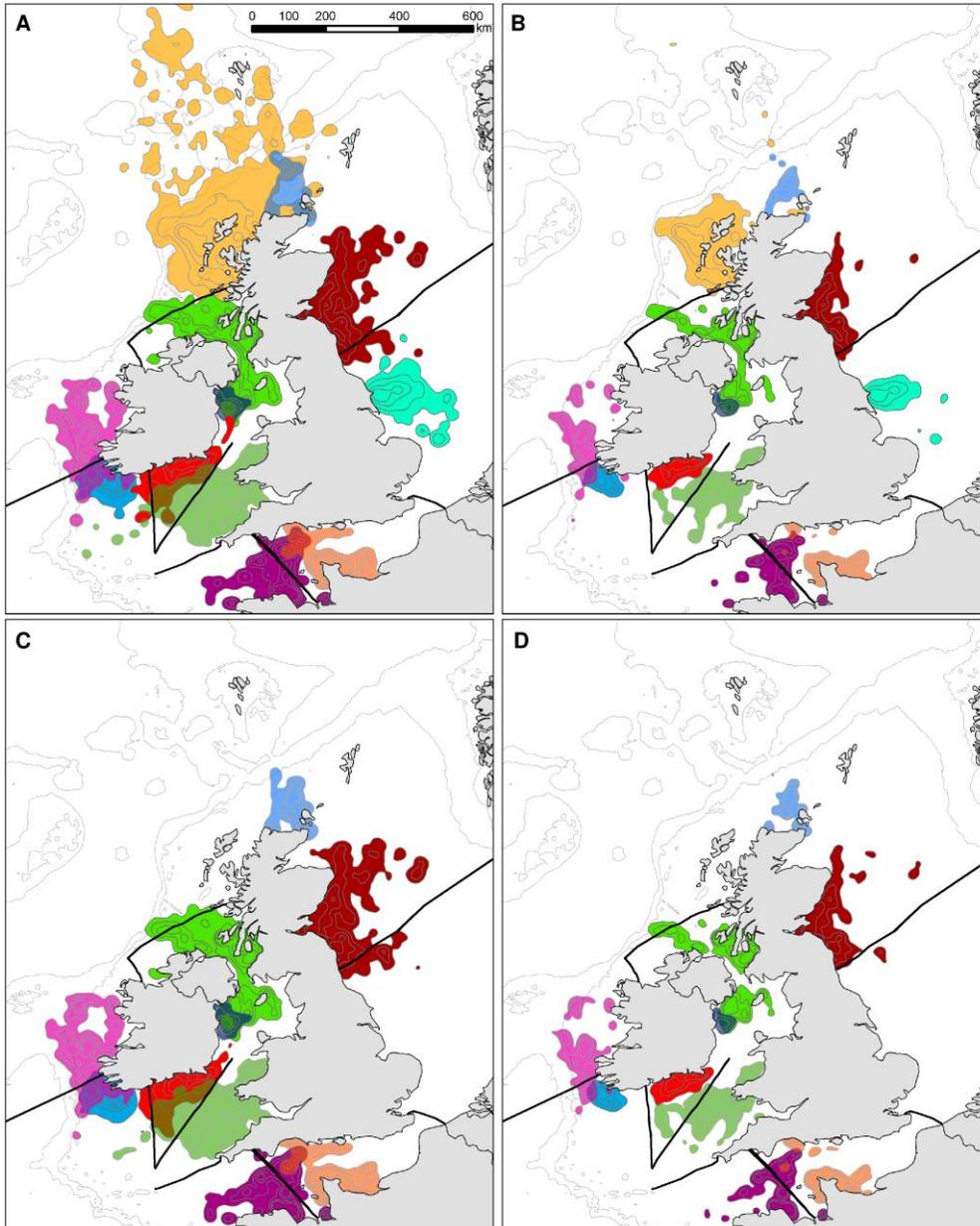
Fig. S2.

Percentage utilization distribution (UD), averaged across individuals within colonies for all tracking locations (**A** 95% and **B** 75% UD) and putative foraging locations only (**C** 95% and **D** 75% foraging UD). Note that c and d show only birds tracked with GPS loggers, as the resolution of PTT data were too coarse to distinguish putative foraging. Contours within the polygons show the extent of the 75, 50 and 25% UDs. Bold black lines show lines of equidistance between pairs of study colonies that are adjacent to one another and have no intermediate colonies. Grey lines indicate the 200 and 1000 m isobaths. Data shown are from 2011, except those for St Kilda, which are from 2010.

11
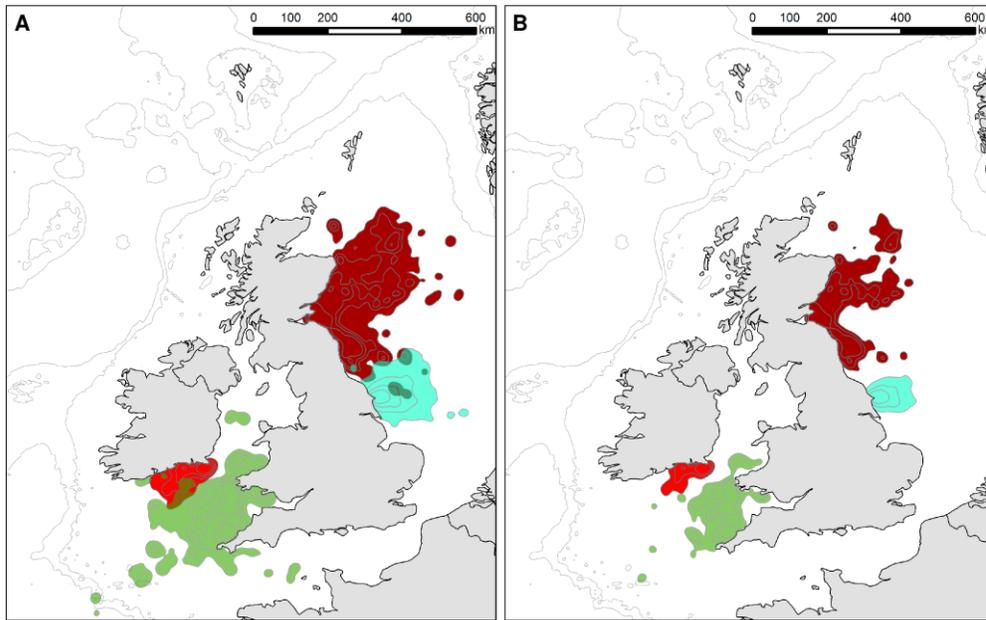
Fig. S3.

Percentage utilization distribution (UD), averaged across individuals within colonies for all tracking locations (**a** 95% and **b** 75% UD) from pairs of colonies in the North Sea (Bass Rock and Bempton) and Celtic Sea (Great Saltee and Grassholm) in 2010. The distribution and degree of between-colony segregation is qualitatively the same as that in 2011 (c.f. Fig. S2A). Contours within the polygons show the extent of the 75, 50 and 25% UDs. Grey lines indicate the 200 and 1000 m isobaths.
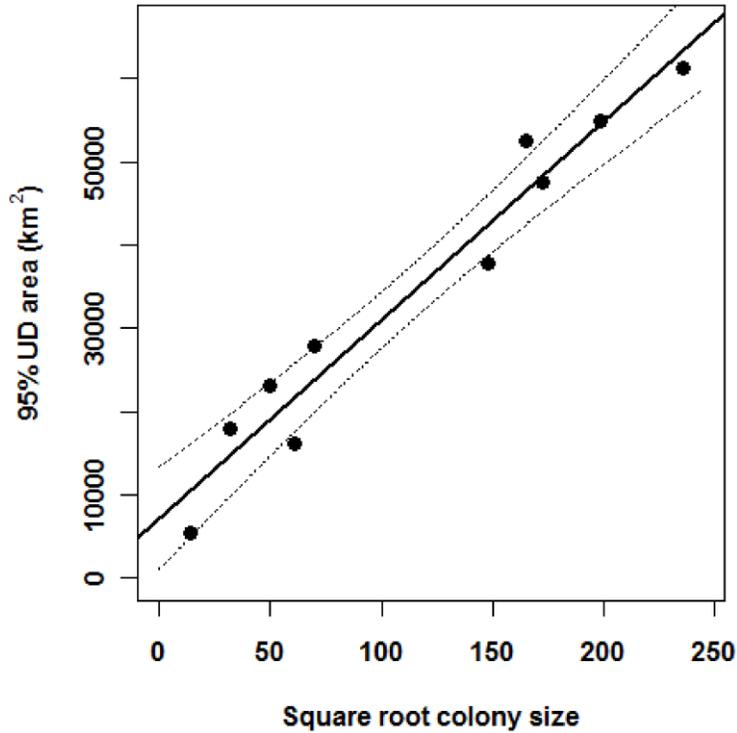
Fig. S4.

Gannets from larger colonies travel further and forage over wider areas. There is a strong relationship between the extent of the colony home range (95% UD illustrated) and square-root colony size (UD area = 7224 + 238 x col size$^{0.5}$). There was a similar relationship at all percentage UDs considered (50, 75 and 95%). Dashed lines indicate 95% CIs. Data are from 2011.
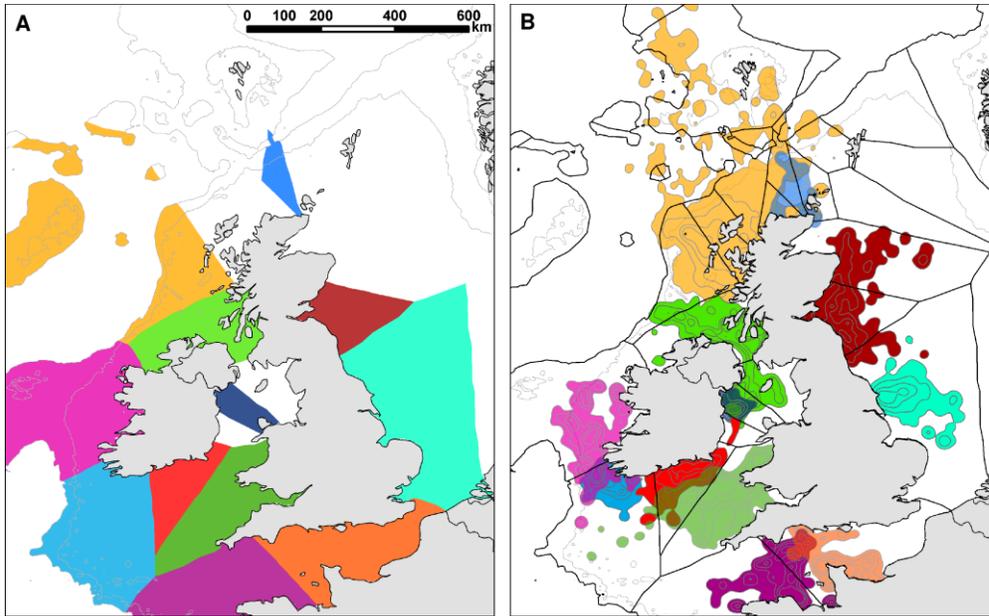
Fig. S5.

Colored polygons show the home ranges (Voronoi polygons) of study colonies predicted by the hinterland model (**A**). The grey line indicates the 200 m isobath. For comparison, Fig. 2A, which shows the observed percentage Utilization Distributions (UDs) of tracked gannets, is reproduced in panel (**B**), with the home ranges of all colonies in the study area predicted by the hinterland model superimposed. Contrary to the hinterland model, there is no relationship between the size of the 37 gannet colonies in the Eastern Atlantic and their respective Voronoi polygon areas, regardless of whether all accessible habitat is considered ($F_{1,35} < 0.01$, p = 0.699, $R^2 < 0.01$) or just neritic waters (i.e. waters < 1000 m deep, $F_{1,35} = 0.01$, p = 0.754, $R^2 < 0.01$). Data shown are from 2011, except those for St Kilda, which are from 2010. Grey lines indicate the 200 and 1000 m isobaths.
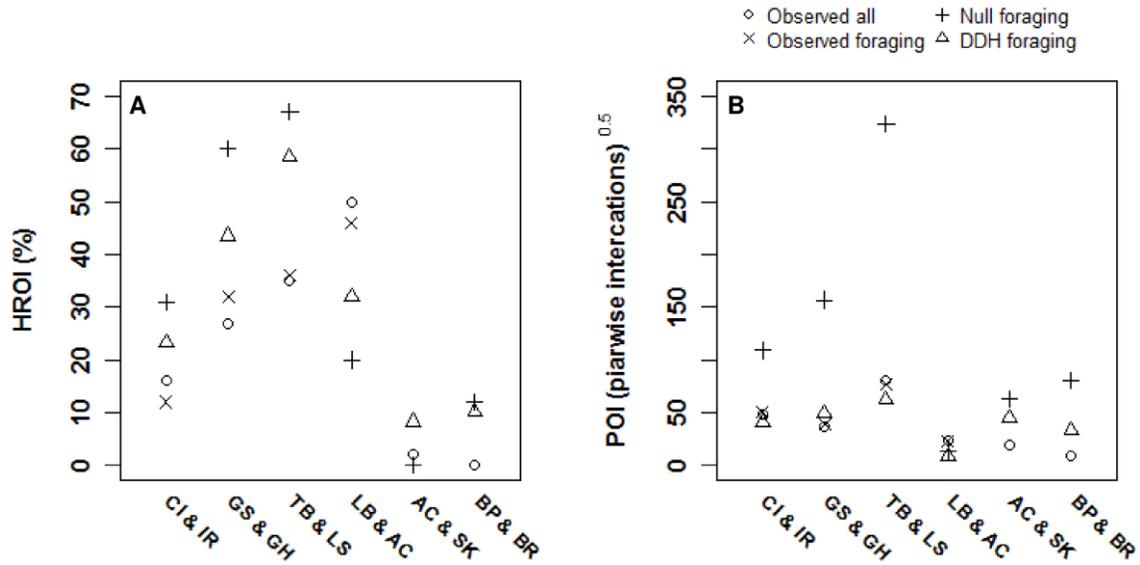
Fig. S6.

Observed and predicted Utilization Distributions (UDs) of gannets from pairs of neighboring colonies (i.e. those adjacent to one another, with no intermediate colonies, see Fig. S2). **A** the Home Range Overlap Index (HROI) between colony 95% UD polygons, while **B** the Population Overlap Index (POI) between colony UDs (see Materials and Methods). Pairs of colonies with zero observed and predicted overlap are not illustrated. Observed UDs were estimated using either *all* tracking locations or putative *foraging* locations alone. The latter were identifiable using GPS tracking data but not PTT data, due to its lower spatiotemporal resolution. Hence, observed overlaps are not presented for birds from St Kilda and Bempton, from which birds were tracked using PTTs. Model predictions are for foraging UDs predicted using either the null model, which assumes that foraging range is proportional to colony size or the density-dependent hinterland (DDH) model, which additionally assumes density-dependent competition with birds from other colonies. For colony codes see Table S1. Data shown are from 2011, except those for St Kilda, which are from 2010.

15
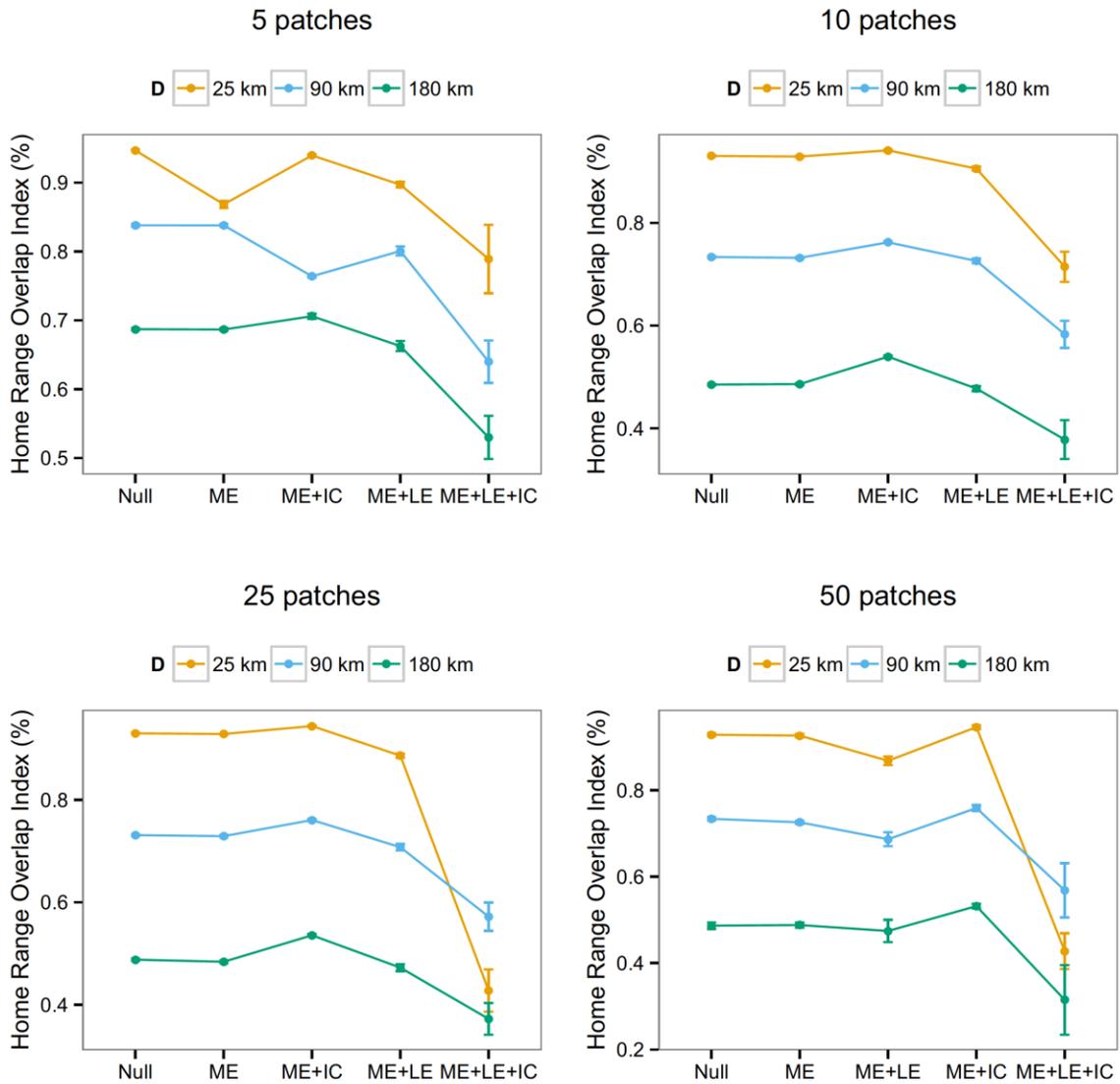
Fig. S7.

Home range overlap indices (HROIs) between 95% Utilization Distributions of two colonies comprising 30 and 300 individuals following 100 simulations of two week time periods. Error bars show 95% CIs. Panels represent different food patch availabilities, with each panel displaying three colony separation distances (25 (orange), 90 (blue) and 190 (green) km). It can be seen that at each forage patch density, it is only when both local enhancement at sea and information transfer at the colony are combined with personal memory (All Sources of Information model - ME +LE+IC), that overlap between home ranges declines significantly.
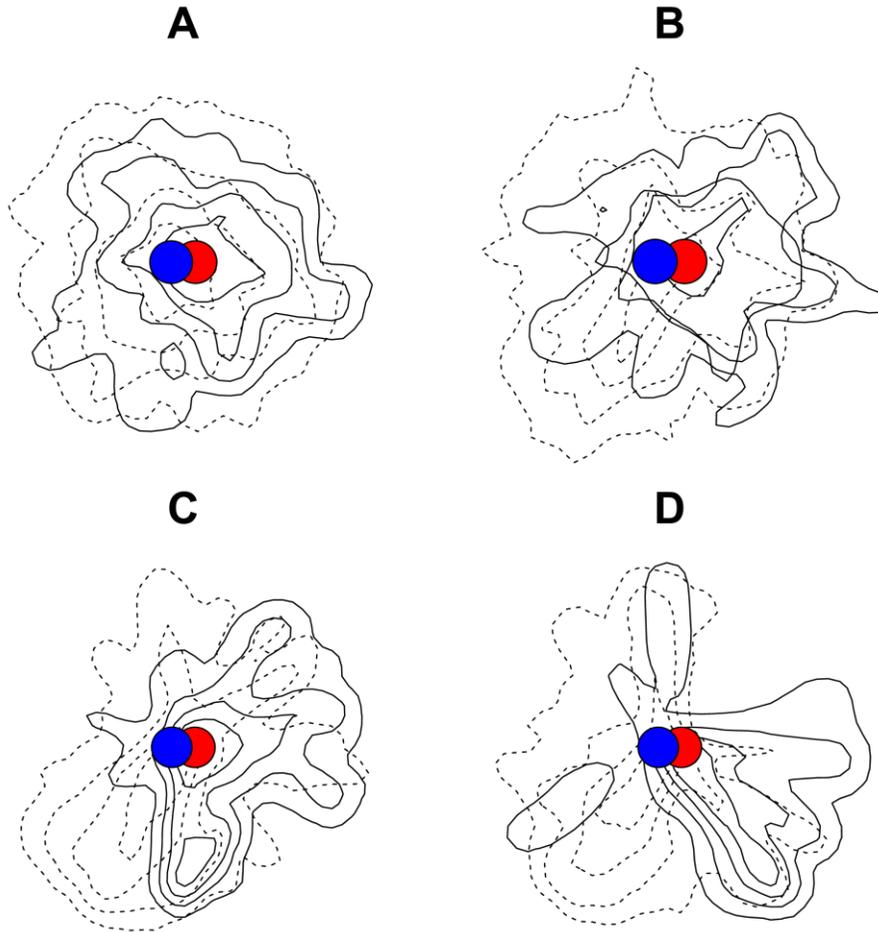
Fig. S8.

Progression through the burn-in period (initial 1000 time steps) for the combined locations from 15 randomly selected simulations of the model incorporating all sources of information (ME + LE + IC): (**A**) time steps 1 – 250; (**B**) time steps 251 - 500; (**C**) time steps 501 – 750; and (**D**) time steps 751 – 1000. Isopleths represent the 50, 75 and 95% UDs of the two colonies, with dashed lines for the smaller colony (red circle), and solid lines for the larger (blue circle). The pattern of colony segregation becomes apparent after 250 time steps. Results are illustrated for simulations involving 50 food patches and 25 km colony separation but were similar for all other parameterizations.
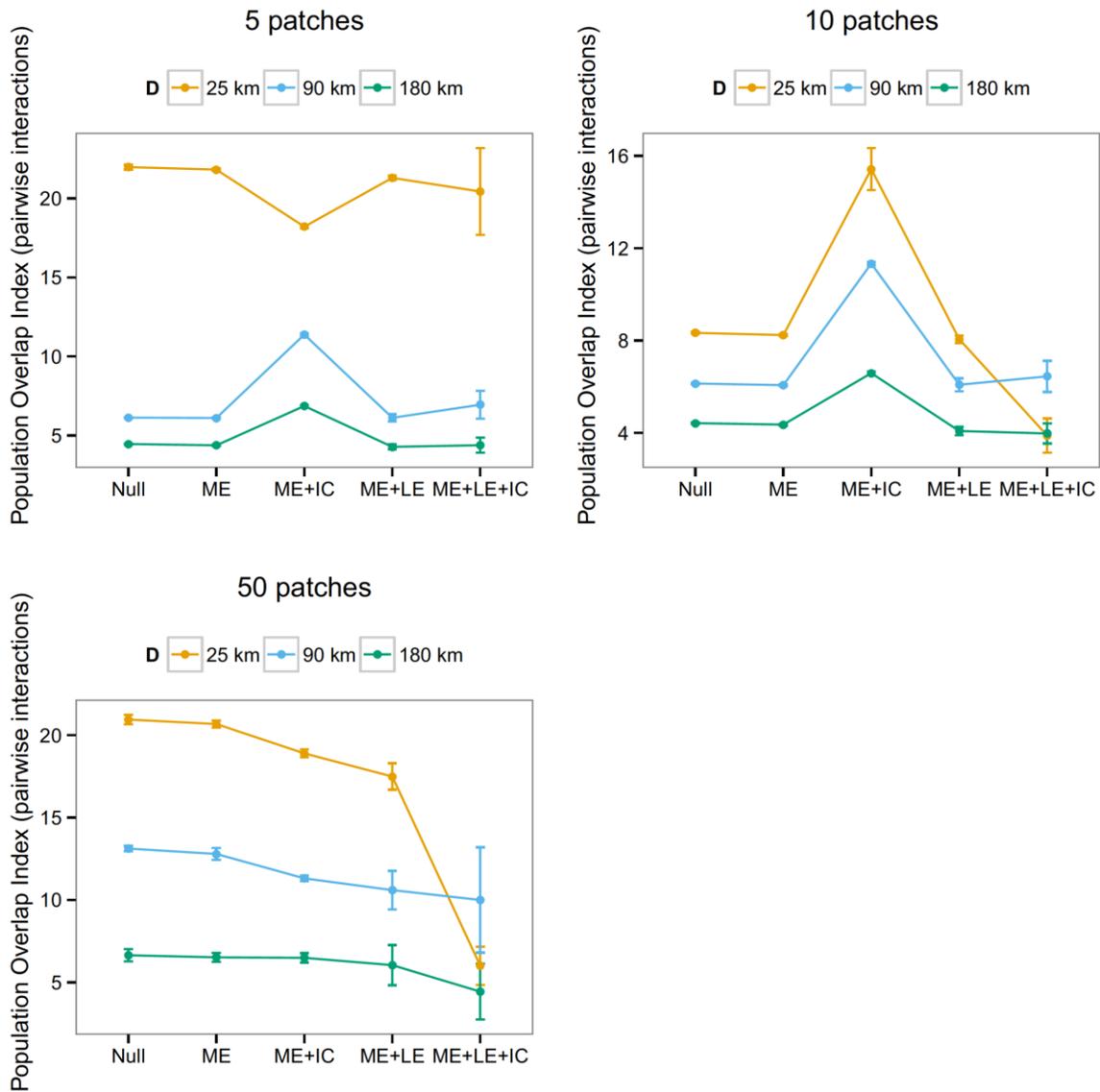
Fig. S9.

Population Overlap Indices (POIs) between utilization distributions of two colonies comprising 30 and 300 individuals following 100 simulations of two week time periods. Error bars show 95% CIs. Panels represent different food patch availabilities, with each panel displaying three colony separation distances (25 (orange), 90 (blue) and 190 (green) km). At very low forage patch density, information use does not result in between colony segregation. However, when patch density increases towards more biologically realistic levels (see also Fig.3) the combination of local enhancement at sea and information transfer at the colony, together with personal memory (All Sources of Information model - ME +LE+IC), results in significantly reduced UD overlap.
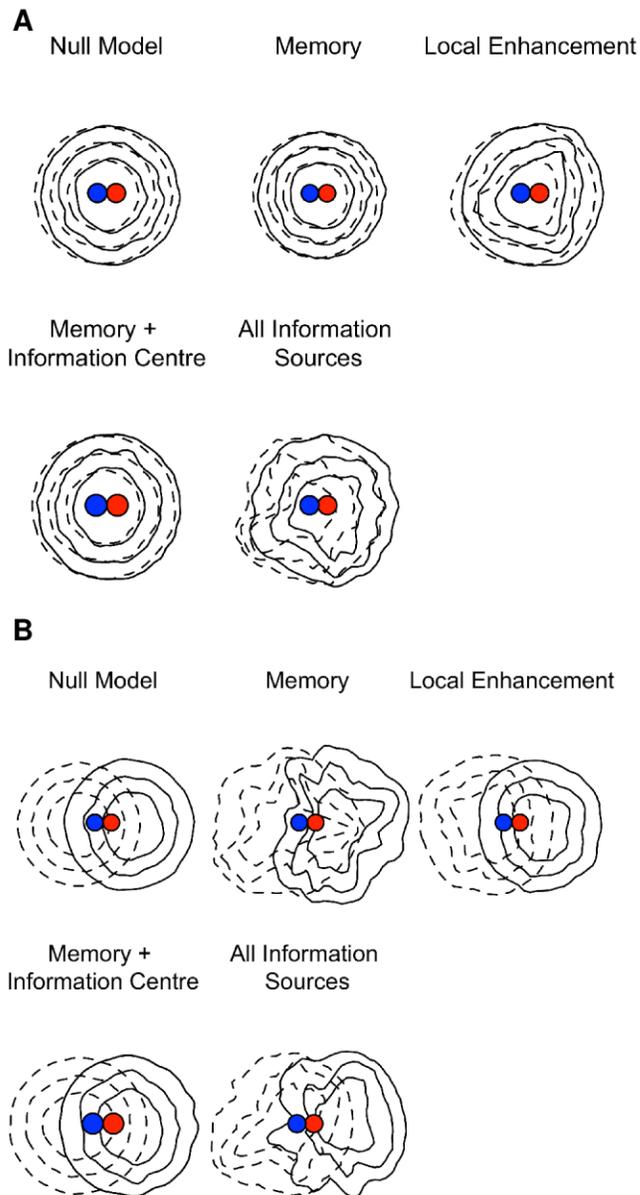
Fig. S10.

Patterns of between-colony segregation simulated by individuals using different sets of behavioral rules at two extremes of separation distances and food patch density. (**A**) 5 patches and 25 km separation (**B**) 50 patches and 180 km separation. Isopleths represent the 50, 75 and 95% UDs of the two colonies, with dashed lines for the small colony (red circle), and solid lines for the larger (blue circle). Colony locations are represented by the red and blue circles respectively. Other combinations of separation and patch density produce qualitatively similar patterns.
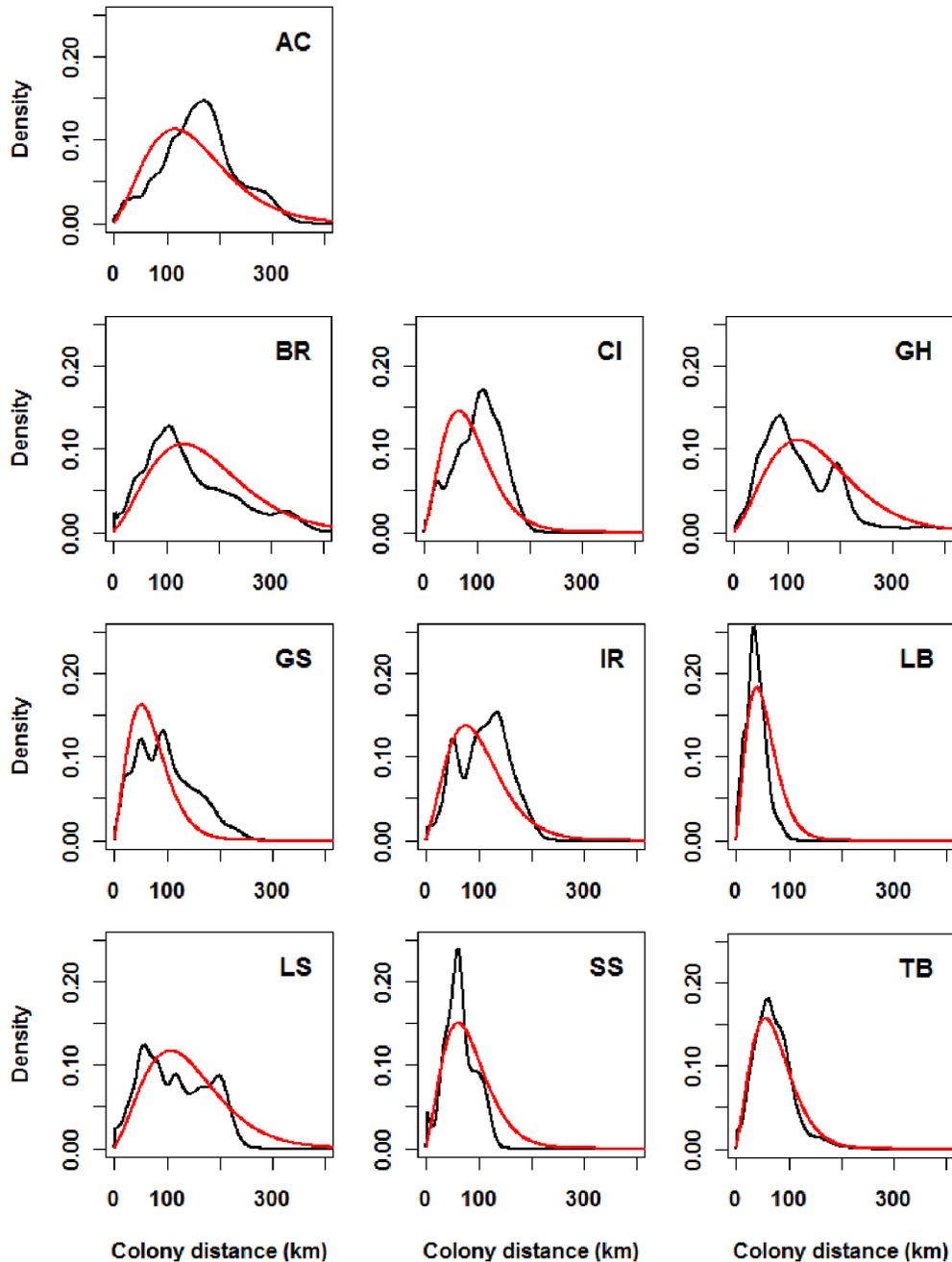
Fig. S11.

The observed distribution of foraging effort with respect to colony distance was right-skewed. Black lines indicate kernel density averaged over individuals within colonies, while red lines show the probability density approximated by the square-root normal distribution used in models 1 and 2. The mean μ_i and standard deviation σ_i of the underlying normal distribution were predicted using empirical relationships with colony size. For colony codes see Table S1. Data shown are from 2011, except those for St Kilda, which are from 2010.
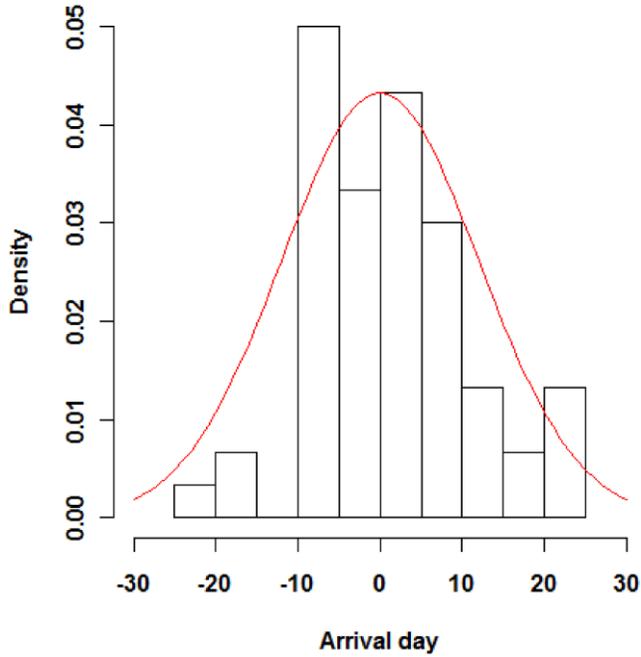
Fig. S12.

Distribution of arrival dates (defined as first night spent in the colony) of northern gannets at Bass Rock at the onset of the breeding season (n = 34 and 27 in 2011 and 2012 respectively). Arrival date is mean-centered within year (mean arrival dates were March 14 in 2011 and March 2 in 2012; overall standard deviation 10 days). The red line indicates the distribution of gannet arrival dates assumed in the density-dependent hinterland model.
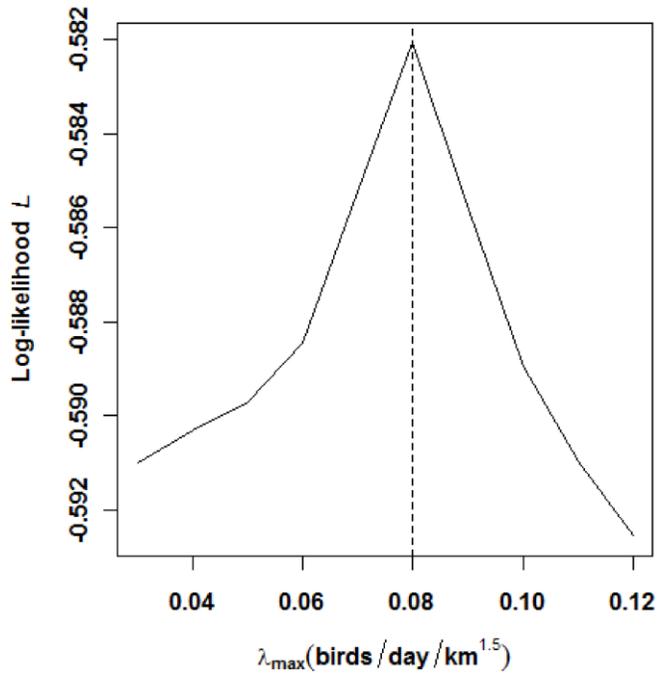
Fig. S13.

Goodness of fit (mean log-likelihood) of the density-dependent hinterland model of fine scale spatial distribution of northern gannet foraging effort with different maximum distance-weighted exploitation rate parameters (λ_{max}). The density-dependent hinterland model performed best when λ_{max} was 0.08 birds/day/km$^{1.5}$ (dashed line).

Table S1.

Study colonies and tracking devices.

Colony†	Code	Location	Colony size N		Tracking device		Birds tracked		Median tracking interval, s (inter-quartile range)‡	TDR
			AOS	Source	Type	Model	2010	2011		2011
Île Rouzic	IR	48º 54' N, 003º 26' W	21,880	LPO	GPS	CatTraQ		21	133 (129-137)	Y
Les Etacs & Ortac	CI	49º 42' N, 002º 14' W	7,409	JNCC	GPS	i-gotu-120		17	129 (123-134)	N
Bull Rock	TB	51º 35' N, 010º 18' W	3,694	Ref (46)	GPS	i-gotu-200		14	117 (113-119)	N
Grassholm	GH	51º 44' N, 005º 29' W	39,292	JNCC	GPS	i-gotu-200	21	26	116 (112-119)	Y
Little Skellig	LS	51º 47' N, 010º 30' W	29,683	Ref (46)	GPS	e-obs GPS-RF		9	120 (118-123)	N
Great Saltee	GS	52º 07' N, 006º 37' W	2,446	JNCC	GPS	i-gotu-200	17	18	116 (113-119)	Y
Lambay	LB	53º 30' N, 006º 00' W	187	JNCC	GPS	i-gotu-200		3	116 (112-119)	N
Bempton	BP	54º 09' N, 000º 10' W	11,061	RSPB	PTT	PTT100/LC4	14	9	2700 (1200-5041)	N
Ailsa Craig	AC	55º 15' N, 005º 07' W	27,130	ref (46)	GPS	e-obs GPS-RF		16	120 (118-122)	N
Bass Rock	BR	56º 05' N, 002º 39' W	55,482	ref (47)	GPS	i-gotu-200	41	28	122 (119-124)	Y
St Kilda	SK	57º 52' N, 008º 29' W	59,800	ref (47)	PTT	Kiwisat202	21		2755 (993-5843)	N
Sule Skerry	SS	59º 05' N, 004º 24' W	1,000	JNCC	GPS	i-gotu-200		2	123 (119-125)	N

AOS = Apparently Occupied Sites, which is considered equivalent to breeding pairs (size estimates for colonies at which no tracking took place are presented in the data supplement); TDR = Time Depth Recorder; JNCC = Joint Nature Conservation Committee seabird monitoring program database (http://jncc.defra.gov.uk/smp/); RSPB = The Royal Society for the Protection of Birds; LPO = Ligue Pour la Protection des Oiseaux; † GPS loggers were also deployed at Scare Rocks (54º 40' N, 004º 42' W) but persistent poor weather prevented their retrieval; ‡ After re-sampling.

Table S2.

Summary of fixed effects in a linear mixed-effects model of double-square-root duration (hours) of the first foraging trip recorded for each satellite-tracked gannet.

Parameter	Estimate (95% CI†)	d.f.†	t-value	p
Intercept	1.796 (1.664, 1.928)	172	26.797	<0.001
Square-root colony size (pairs) x 10^{-3}	1.729 (0.807, 2.651)	10	4.179	0.002

†Approximate estimates; N.B. Colony was treated as a random effect.

Table S3.

Summary of fixed effects in a linear mixed-effects model of double square-root maximum distance[‡] from the colony (km) reached during the first foraging trip recorded for each satellite-tracked gannet.

Parameter	Estimate (95% CI[†])	d.f.[†]	t-value	p
Intercept	2.734 (2.517, 2.952)	172	24.821	<0.001
Square-root colony size (pairs) x 10^{-3}	3.546 (2.023, 5.069)	10	5.190	<0.001

‡ Shortest path distance avoiding land; †Approximate estimates; N.B. Colony was treated as a random effect.

Table S4.

Summary of fixed effects in a linear mixed-effects model of log individual mean time in colony/time at-sea spent by gannets tracked for ≥ trips.

Parameter	Estimate (95% CI†)	d.f.†	t-value	p
Intercept	0.012 (-0.186, 0.211)	111	0.123	0.902
Square-root colony size (pairs)	-0.0008 (-0.0021, - 0.0005)	8	-1.429	0.191

†Approximate estimates; N.B. Colony was treated as a random effect.

Table S5.

Summary of fixed effects in a linear mixed-effects model of log mean n foraging trips/day made by gannets tracked for ≥ trips.

Parameter	Estimate (95% CI†)	d.f.†	t-value	p
Intercept	0.039 (-0.166, 0.243)	111	0.376	0.708
Square-root colony size (pairs)	-0.002 (-0.003, -0.002)	8	-2.786	0.023

†Approximate estimates; N.B. Colony was treated as a random effect.

Table S6.

Goodness of fit of two models of the coarse scale spatial distribution of northern gannet foraging effort.

Colony	log-likelihood, L	
	Hinterland	Null model
Île Rouzic	-1.03	**-0.26**
Les Etacs & Ortac	-0.45	**-0.32**
Bull Rock	-0.32	**-0.24**
Grassholm	-0.61	**-0.29**
Little Skellig	**-0.51**	-0.52
Great Saltee	-0.44	**-0.38**
Ailsa Craig	-0.90	**-0.37**
Lambay	**-0.16**	-0.27
Bass Rock	-0.89	**-0.33**
Sule Skerry	-0.09	**-0.01**
Mean	-0.54	**-0.30**

Values in bold indicate maximum log-likelihood.

Table S7.

Goodness of fit of two models of fine scale spatial distribution of northern gannet foraging effort.

Colony	Log-likelihood, L	
	Null model	Density-dependent hinterland model
Île Rouzic	-0.65	**-0.63**
Les Etacs & Ortac	-0.69	**-0.67**
Bull Rock	-0.56	**-0.44**
Grassholm	-0.56	**-0.52**
Little Skellig	-0.54	**-0.52**
Great Saltee	-0.68	**-0.62**
Ailsa Craig	-0.66	**-0.65**
Lambay	**-0.59**	-0.63
Bass Rock	-0.51	**-0.49**
Sule Skerry	-0.68	**-0.64**
Mean	-0.61	**-0.58**

Values in bold indicate maximum log-likelihood.

Table S8.

Similarity between observed foraging Utilization Distributions and those predicted by the null and Density-Dependent Hinterland (DDH) models.

Colony	Dice's Similarity Coefficient s			
	UD_{75}		UD_{95}	
	Null	DDH	Null	DDH
Île Rouzic	0.41	**0.42**	0.70	**0.71**
Les Etacs & Ortac	0.28	**0.29**	0.49	**0.56**
Bull Rock	0.39	**0.77**	0.57	**0.76**
Grassholm	0.56	**0.58**	0.68	**0.70**
Little Skellig	0.57	**0.60**	**0.62**	0.59
Great Saltee	0.50	**0.60**	0.51	**0.60**
Ailsa Craig	0.39	**0.45**	0.69	**0.74**
Lambay	0.50	**0.55**	0.69	**0.74**
Bass Rock	0.69	**0.70**	**0.69**	0.69
Sule Skerry	0.22	**0.44**	0.53	**0.65**
Median	0.45	**0.57**	0.65	**0.70**

UD = Utilization Distribution. Values in bold indicate the model whose predicted UD was most similar to that observed.

Table S9.

Constraints applied to individual-based simulations of gannet foraging behavior.

Parameter	Value	Reference
Maximum foraging range	525 km	(*48*)
Average foraging range	236 km	(*49*)
Maximum detection distance of unexploited patch	5 km†	(*50*)
Maximum detection distance of exploited patch	20 km†	(*50*)
Maximum detection distance of knowledgeable birds at sea	10 km†	(*50*)
Maximum detection distance of knowledgeable birds in the vicinity of the colony	10 km†	(*50*)

†Detection distances are placed towards the higher end of the detection spectrum based on the large size, striking plumage and highly visible wheeling and plunge-diving feeding behaviors of gannets. Reducing these terms increases the importance of information transfer in the vicinity of the colony as fewer individuals detect each other at sea.

Table S10.

Rules incorporated in individual-based simulations of gannet foraging behavior.

Foraging rules	Description
Null	Individuals forage randomly every time they leave the colony but avoid areas with a high density of conspecifics when > 50km from their own colony (densities are always high in the vicinity of colonies).
+ ME (Memory)	In addition, individuals return to a known food patch following successful previous foraging (private information). Individuals will use private information in preference to reducing local densities.
+ ME + LE (Local Enhancement)	In addition, uninformed individuals can observe and follow knowledgeable individuals at sea heading towards a known destination (public information gain at sea).
+ ME + IC (Information Centre)	As with above, but individuals observe and follow knowledgeable individuals from the vicinity of the colony only (public information gain at colony).
+ ME + LE + IC	Uninformed individuals can observe and follow knowledgeable individuals both from the vicinity of the colony and at sea (full use of public and private information).